Nanochem Res 8(3): 164-172 Summer 2023

RESEARCH PAPER

Cuminum Cyminum L Encapsulation on Perlite/calcium alginate/single walled carbon nanotubes -Glucose Composite: Fabrication, Characterization, Antibacterial and Antifungal Properties

Mahdieh Chegeni*, Mozhgan Mehri, Zahra Shokri Rozbahani

Department of Chemistry, Ayatollah Boroujerdi University, Boroujerd, Iran

ARTICLE INFO

Article History:
Received 16 Nov 2022
Accepted 21 May 2023
Published 27 May 2023

Keywords:
Antibacterial
Biomaterial
Cumin
Encapsulation
perlite/calcium alginate/SWCNT-Gl

ABSTRACT

This study presents the preparation and application of a perlite/calcium alginate/single walled carbon nanotubes-Glucose composite for the cumin encapsulation as an essential oil using a simple method. The as-prepared composite was analyzed using Fourier transformed infrared (FTIR), field emission scanning electron microscopy (FESEM), X-ray diffractometer (XRD), dynamic light scattering (DLS), and thermo gravimetric analysis (TGA). The effect of important factors was determined by evaluating pH, cumin concentration, perlite/calcium alginate/single walled carbon nanotubes-Glucose dosage, and time. Based on the data, the high percentage of cumin encapsulation was achieved at low pH. The release profile of cumin was studied at pH=7, and the maximum release was obtained after 48 h. The antibacterial and antifungal properties of cumin-loaded perlite/calcium alginate/single walled carbon nanotubes -Glucose were also evaluated against *Candida albicans*, Gram negative (*Escherichia coli*) and Gram positive (*Staphylococcus aureus*) bacteria, which represented more photogenic detection compared to that of cumin. Finally, this work demonstrates the efficient application of perlite/calcium alginate/single walled carbon nanotubes-Glucose for the encapsulation of cumin and pathogen detection.

How to cite this article
Chegeni M., Mehri M., Shokri Rozbahani Z., Cuminum Cyminum L Encapsulation on Perlite/calcium alginate/single walled carbon nanotubes -Glucose Composite: Fabrication, Characterization, Antibacterial and Antifungal Properties. Nanochem Res, 2023; 8(3): 164-172 DOI: 10.22036/ncr.2023.03.001

INTRODUCTION

Essential oils are interesting molecules with a variety of applications, including antifungal, antibacterial, and natural additives of food products [1]. They are extensively used in food chemistry for decreasing oxidative reactions, as opposed to synthetic additives [2].

Cumin as an essential oil is widely used in aromatherapy applications, food, and pharmacology systems, and it is applied as a medicine in many cultures. Further, studies have shown that cumin can be effective in decreasing pain without side effects. However, its hydrophobic and volatility properties can limit its use in food, cosmetic, and pharmacologic industries [3].

To overcome the problem of using essential oils (Eos), encapsulation is suggested as a viable approach to modify their characteristics. A large number of materials have been reported for loading drugs and essential oils such as cyclodextrins [4], sodium alginate [5], porous silica and MOFs [6], chitosan [7], modified dextran-coated superparamagnetic iron oxide [8], and liposomes [9]. However, some of the reported methods have been found to have issues including low solubility, oxidation, and low efficiency [7]. Thus, the design of more efficient compounds is necessary to improve

* Corresponding Author Email: *mahdieh.chegeni@abru.ac.ir*

loading. Polymer nanoparticles have been gaining attention from researchers for loading of Eos due to their high yield.

In recent years, the development of green chemistry has led to the use of natural materials as efficient and low-cost compounds for the synthesis of novel system materials. Furthermore, researchers have introduced biocomposites as a new class of materials and applied in various fields. Biopolymers are an important category of compounds that can be used in different industries with minimal environment impact. While biopolymers have been reported to have several advantages, they have been found to have some limitations in chemical stability and mechanical properties. To address these problems, the addition of fillers can be used to modify the structure of biopolymers.

Polysaccharides are an attractive class of biopolymers due to their low-cost, biodegradablity and sustainability, making them suitable for use in many industries such as food, textile, and pharmaceuticals. To improve the mechanical properties of polysaccharides, many materials have been used including polycaprolactone/starch [10], starch-chitosan [11], starch-chlorogenic acid [12], dicarboxylic acid modified starch-clay composite [13], and graphene oxide/Bi_2WO_6/starch composite [14]. Thus, the selection of a suitable filler is essential for optimizing the performance of biopolymers.

Alginate, a biopolymer obtained from algae, has been of great interest due to its ability to form hydrogels by replacing cations, as demonstrated by the "egg box" model [15]. Its stability and existence of functional groups have enabled its use in a variety of applications, such as metal ion support [16], tissue engineering [17], drug delivery [18], 3D bioprinting [15], food chemistry [19], and adsorption [20].

The use of carbon nanotube (CNT) can be an attractive option as a filler due to its advantageous characteristics. CNTs have been used in many fields such as biomedicine, electronics, catalysis, drug delivery, and ceramics [21]. However, the van der Waals force present in CNT can lead to low solubility and biocompatibility, which can negatively impact the performance of polymers. To address this issue, several biomolecules were applied such as glucose [22], calcium alginate [23], and vitamin C [24].

In addition, clay can be employed as an effective filler to obtain the most favorable interaction with various compounds. Perlite can be achieved from natural resources composed of alumina and silanol groups with high surface area, ion exchange capability, and low weight. The functional groups of perlite surface can bond with other materials and improve the properties of compounds. Perlite as a volcanic glass has been applied in several fields such as construction [25], catalysis [26], adsorption [27], and drug delivery [28], and its advantages can offer new perspectives for modifying composite properties.

Based on the reported literature, calcium alginate/SWCNT-Gl has been used as a nanocarrier for drug delivery [23]. To improve its properties and enable encapsulation of essential oils, perlite was added to the as-prepared nanocomposite and the components were attached via various interactions such as ester and hydrogen bonds. The formation of the as-prepared biopolymer was confirmed by X-ray diffractometer (XRD), Fourier transformed infrared (FTIR), dynamic light scattering (DLS), thermo gravimetric analysis (TGA), and field emission scanning electron microscopy (FESEM) analysis. The obtained biopolymer was then evaluated for the encapsulation of cumin as an essential oil, and the effects of pH, cumin concentration, biocomposite dose, and time were examined. The pathogenicity of cumin-loaded on perlite/calcium alginate/SWCNT-Gl (P/CA/SWCNT-Gl) was studied against *Escherichia coli* (*E. coli*), *Staphylococcus aureus* (*S. aureus*), and *Candida albicans*. This work reports the ability of as-prepared composite for the encapsulation of cumin, which can be used to overcome the limitation of cumin-loaded in drug delivery and food chemistry. The process uses simple, inexpensive, and natural compounds.

EXPERIMENTAL METHOD

Materials and methods

Sodium alginate, *N,N′*-carbonyl diimidazole (CDI), calcium chloride ($CaCl_2$), hydrochloric acid (HCl), sodium hydroxide (NaOH), and phosphate-buffered saline (PBS) were purchased from Merck and Sigma-Aldrich Chemical Companies, and were used without any purification. In addition, carboxyl-modified SWCNTs (diameter 8 nm, length 10–30 μm) were purchased from Neutrino Co. (Tehran, Iran), and perlite was obtained from Mashhad mine, Iran.

Cuminum Cyminum L was supplied from Barig Essence Pharmaceutical Co, Iran. The *Cuminum Cyminum L* contained α-pinene (1.63%), cumin

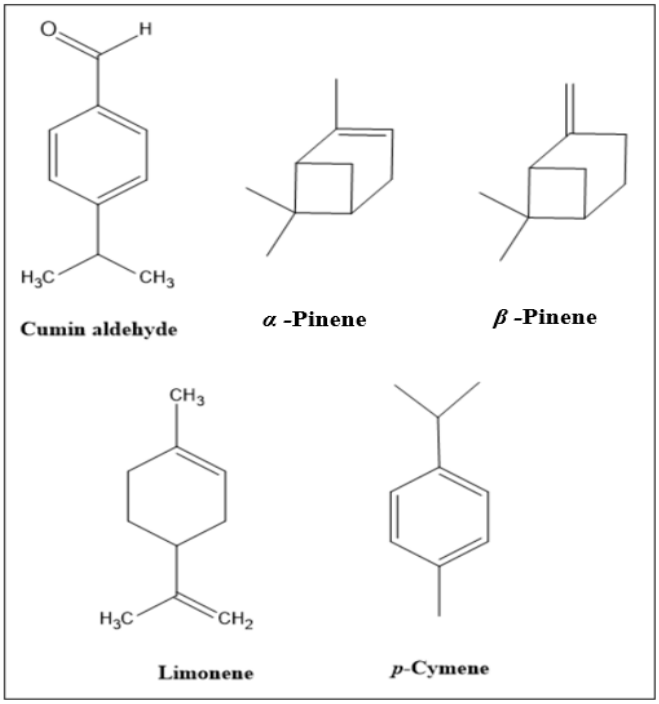

Scheme 1. Chemical composition of *Cuminum Cyminum L.*

aldehyde (29.84%), *β*-pinene (15.05%), limonene (0.82%), and *p*-cymene (16.08%), that their structures are shown in Scheme 1, and cumin aldehyde was the major compound of *Cuminum Cyminum L.*

The functional groups of compounds were determined by Unicam-Galaxy 5000 with KBr pellets, and the morphologies were determined by field emission scanning electron microscopy (FESEM, TescanMira3-Lmu). The crystal phase of compounds was obtained by Panalytical Xpertpro diffractometer using Cu Kα radiation (λ=1.54178 Å). The thermo gravimetric analysis (TGA) was studied by the use of Q600-TA (Unit State) with the scan range from 25 °C to 800 °C under N_2 atmosphere with the constant heating rate of 20 °C/min. A Zeta-sizer Zen 3600 instrument was achieved by Horiba, SZ100, Japan.

Preparation of perlite/calcium alginate/SWCNT-Gl composite

The calcium alginate/SWCNT-Gl was prepared according to Ref [28]. Initially, 0.002 g of CDI was dissolved in distillated water, followed by the addition of 0.024 g carboxyl-modified SWCNTs and stirred for 2 h, and 0.045 g *D*-glucose was mixed and ultrasonicated for 2 h. Sodium alginate was then added to the obtained precipitation (SWCNT-Gl), and was ultrasonicated for 1h. To achieve the calcium alginate/SWCNT-Gl, $CaCl_2$ (1 % w/v) was dropped granularly, and pure perlite was added to the obtained mixture with the ratio of 1:2. The solution was stirred for 1h and ultrasonicated for 2h. Finally, the precipitation was characterized by several analyses.

Cumin-loaded in the perlite/calcium alginate/ SWCNT-Gl composite

To demonstrate the yield of cumin loading in perlite/calcium alginate/SWCNT-Gl, 0.005 g P/CA/ SWCNT-Gl was added to 6 ppm of cumin at pHs (2-7) for 90 min, and the solution was stirred for 1h, then the mixture was centrifuged. The cumin concentration was measured by UV spectroscopy at 255.5 nm, and entrapment efficiency (EE) was calculated by Equation (1).

$$\text{Entrapment Efficiency } (\%) = \frac{(\text{Total amount of cumin}) - (\text{Free amount of cumin})}{(\text{Total amount of cumin})} * 100 \qquad \text{Eq. (1)}$$

Cumin release study

The release profile of cumin was evaluated at pH=7 and 37 °C in aqueous solution, and the concentration of cumin was obtained by UV–Vis spectrophotometer at 255.5 nm.

Pathogen activity

The paper disk method was applied to study the activity of P/CA/SWCNT-Gl against *Escherichia coli* (*E. coli*, ATCC 10536) and *Staphylococcus aureus* (*S. aureus*, ATCC 29737), and *Candida albicans* (ATCC 10231).

RESULTS AND DISCUSSION

Structural properties

The perlite/calcium alginate/SWCNT-Gl was prepared by a simple strategy, and the cumin was encapsulated as an essential oil. Several techniques were applied to illustrate the preparation of the P/CA/SWCNT-Gl composite.

Fig. 1 presents the functional groups of CA, perlite, *D*-glucose, CA/SWCNT-Gl, and P/CA/SWCNT-Gl composite. In perlite, the peaks at 3445 and 1063 cm^{-1} are assigned to the stretching mode of hydroxyl groups and Si–O–Al (Si–O–Si) bonds. The peak positioned at 3417 cm^{-1} indicates the stretching vibration of hydroxyl groups, as shown in CA spectrum, and the -C-H and C-O bonds are ascribed to the peak at 2930 and 1018 cm^{-1}, respectively. The *D*-glucose FTIR spectrum shows the peaks at 3270, 1437, and 1018 cm^{-1}, which belong to -OH, -C-O-H, and C-O stretching vibrations. The spectrum of CA/SWCNT-Gl provides the bond hydrogen by the peaks at 3000-3500 cm^{-1}. Further, the peaks at 1731, 1404, 1014 cm^{-1} evidence the ester, carboxylate salt, and C-O bonds. Furthermore, the peaks at 3438, 1725, 1392, 1038, 575 cm^{-1} indicate the presence of hydroxyl groups, ester bonds, carboxylate salt, C-O vibration, and Si-O bonds in P/CA/SWCNT-Gl composite. The interactions between components were confirmed by the decrease of wavenumbers intensity.

The X ray diffraction patterns of perlite, SWCNT-Gl, and P/CA/SWCNT-Gl are seen in Fig. 2. The amorphous structure of perlite is shown by presenting the peaks from 2ɵ=16.8° to 2ɵ=28.2°. The pattern of SWCNT-Gl is ascribed to the graphitic carbon peak at 2ɵ =27.9° and (0 0 2). Bragg reflection can be seen in P/CA/SWCNT-Gl pattern. The peaks at 2ɵ=26.2°, 2ɵ =43.0°, and 2ɵ=43.0° are observed in the P/CA/SWCNT-Gl composite which demonstrate the presence of alginate and perlite.

Fig. 3 provides the morphologies of CA/SWCNT-Gl, and P/CA/SWCNT-Gl using FESEM. As seen in Fig. 3a, the CA/SWCNT-Gl images are shown by beads of alginate and *D*-glucose as a white spot on SWNT-COOH. In Fig. 3(b-d), the morphologies of P/CA/SWCNT-Gl and the interaction between components are presented. In addition, the size of P/CA/SWCNT-Gl was increased from 29-43 to 57-76 nm, which confirms the formation of bonds between perlite and CA/SWCNT-Gl composite.

The stability of P/CA/SWCNT-Gl was evaluated by TGA analysis from 25 to 800 °C (Fig. 4). The first region of weight loss is obtained under 180 °C, which was attributed to the presence of H_2O. The second region of TGA, between 200 and 600 °C, showed a 20 % wight loss. Based on the obtained data, 41.33% of CA/SWCNT-Gl weight decreased during degradation [28], while 37.30 % weight loss of P/CA/SWCNT-Gl occurred, suggesting that the as-prepared composite was more stable due to intra- and intermolecular hydrogen bonding.

The DLS analysis of the as-prepared biocomposite revealed a mean diameters (MD) of 211.34 nm and a polydispersity index (PDI) ranging from 0.364 to 0.369 (Fig. 5). This indicates a good distribution of the cumin-loaded P/CA/SWCNT-Gl particles.

The effective parameters, such as pH, cumin concentration, biocomposite dose, and time, were evaluated for the encapsulation of cumin. The zeta potential values were obtained to determine the effect of pH for loading of cumin by P/CA/SWCNT-Gl composite. Based on the results, the -28.4, -38.76, and -46.7 mV values were evaluated for cumin, P/CA/SWCNT-Gl, and cumin-loaded P/CA/SWCNT-Gl. Additionally, the experiments demonstrated the high yield of cumin loading at low pH compared to that of high pH, because the positive charge can increase the interaction between components. Furthermore, the concentrations of cumin (2-18 ppm), composite dosage, and time (1-9 h) were tested, which the highest encapsulation efficiency (EE) was determined to be 66% at 6 ppm of cumin, 0.005 g P/CA/SWCNT-Gl composite, and 8 h.

The release of cumin from the P/CA/SWCNT-Gl composite was performed at 8-48 h, pH=7, and 37 °C similar to the physiological condition of the human body. The highest release was observed after 48 h.

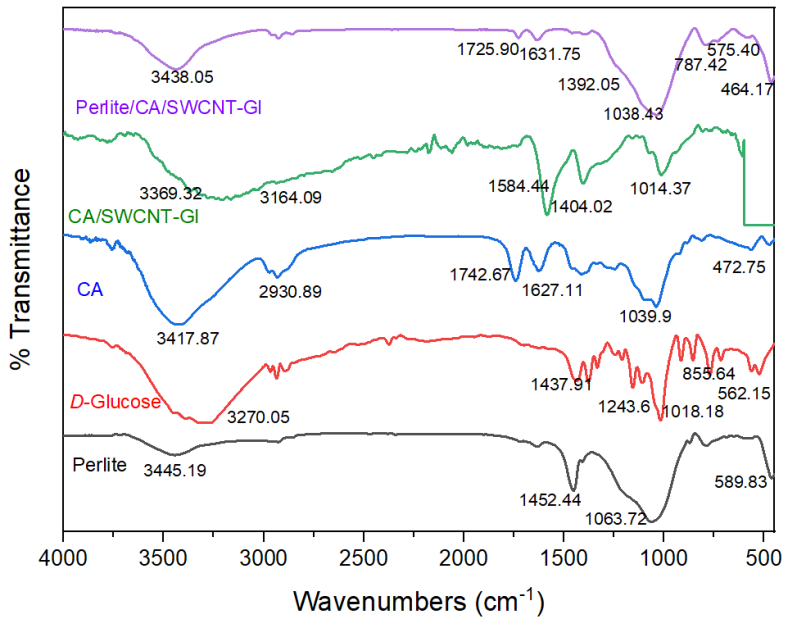

Fig. 1. FTIR spectra of CA, perlite, *D*-glucose, CA/SWCNT-Gl, and P/CA/SWCNT-Gl composite.

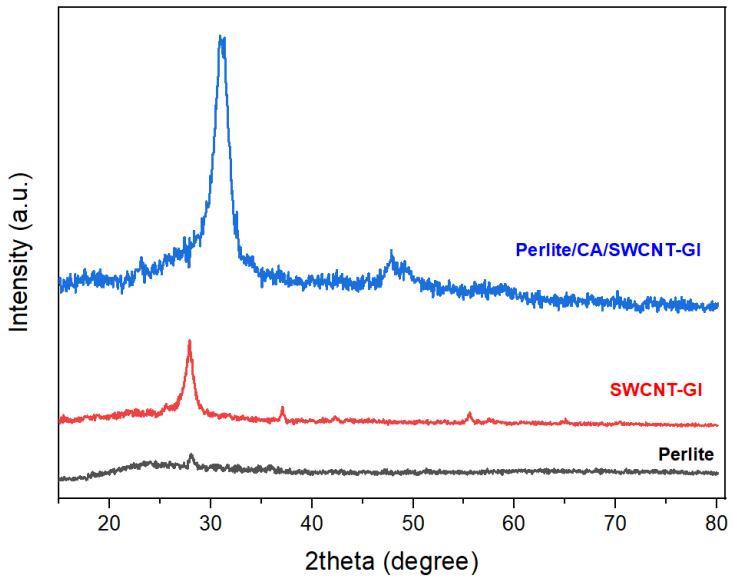

Fig. 2. XRD patterns of perlite, SWCNT-Gl, and P/CA/SWCNT-Gl composite.

Pathogen detection of cumin-loaded P/CA/SWCNT-Gl

The pathogen detection of cumin and cumin-loaded P/CA/SWCNT-Gl was evaluated against Gram negative (*Escherichia coli*), Gram positive (*Staphylococcus aureus*), and *Candida albicans*. In Fig. 6, the activities of cumin and cumin-loaded P/CA/SWCNT-Gl are presented, and their minimum inhibitory concentrations (MIC) are seen in Table 1. Further, the thick well of *Escherichia coli* was observed to have higher MIC value compared to that of *Staphylococcus aureus*. Furthermore, the viable cell count method demonstrated a reduction percentage of more than 99% of bacteria, as shown in Fig. 7. The results suggest that the as-prepared biocomposite can be employed affectively against both bacterial and fungal pathogens.

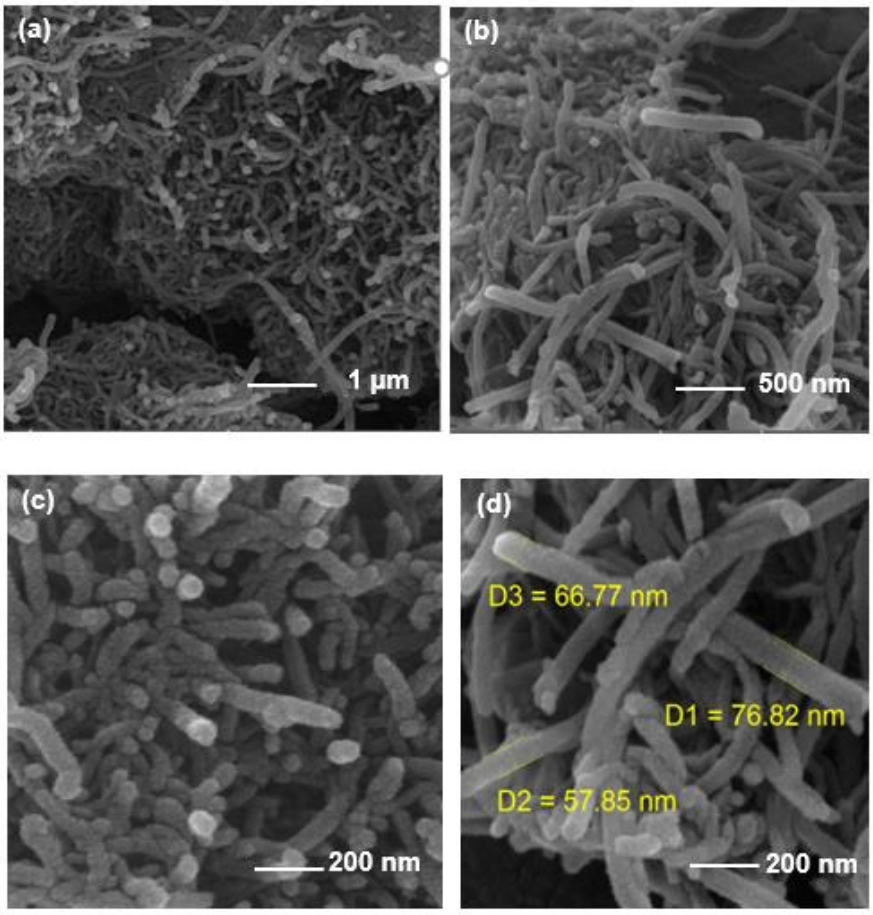

Fig. 3. FESEM images of (a) CA/SWCNT-Gl and (b-d) P/CA/SWCNT-Gl composite.

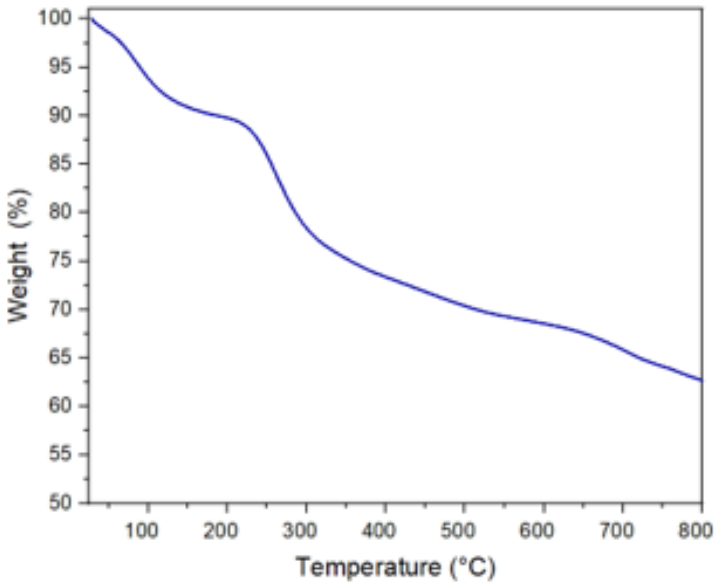

Fig. 4. TGA curve of P/CA/SWCNT-Gl composite.

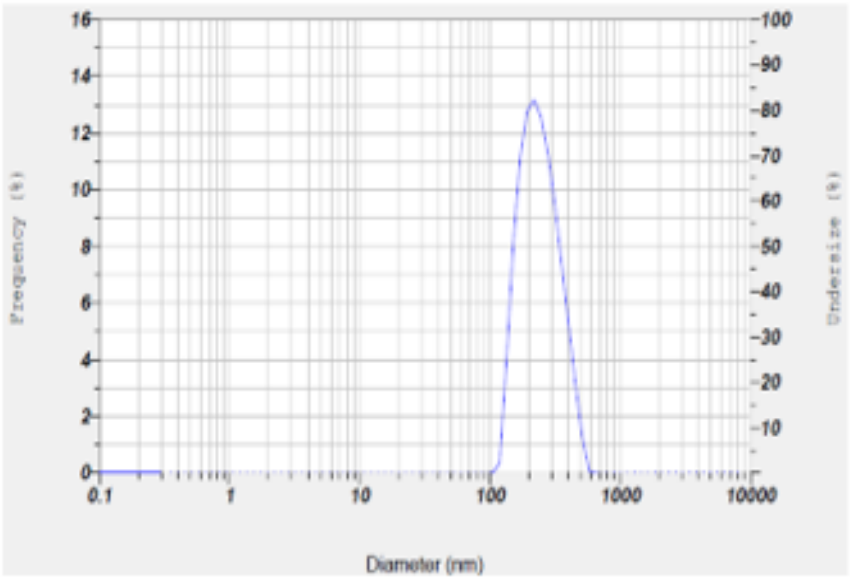

Fig. 5. PSD curve of cumin-loaded P/CA/SWCNT-Gl composite.

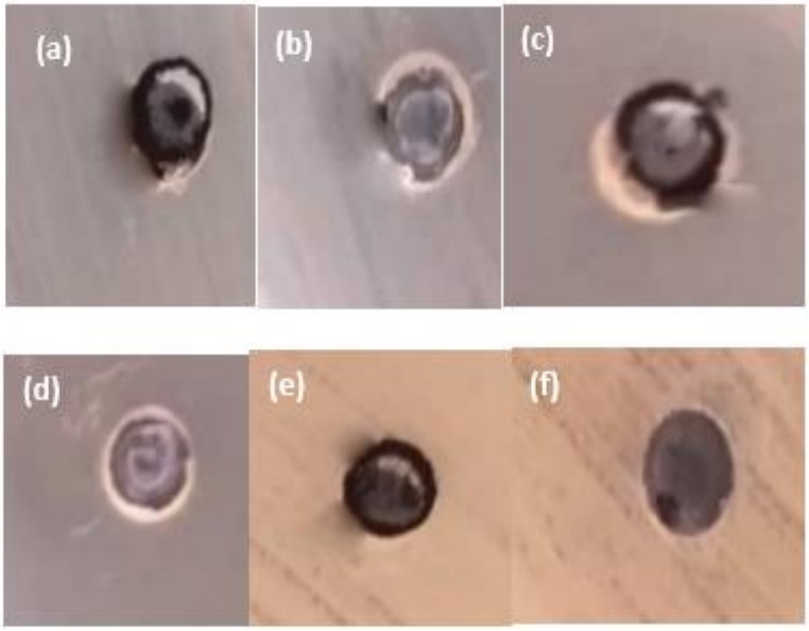

Fig. 6. (a,c,e) Cumin-loaded P/CA/SWCNT-Gl, (b,d,f) cumin against (*S. aureus*), (*E. coli*), and *Candida albicans*.

Table 1. The MIC values of cumin-loaded P/CA/SWCNT-Gl and cumin against pathogen.

Test microorganism	MIC ($\mu g.ml^{-1}$)	MIC ($\mu g.ml^{-1}$)
	Cumin-loaded P/CA/SWCNT-Gl	Cumin
Escherichia coli (ATCC 10536)	500	250
Staphylococcus aureus (ATCC 29737)	62.50	62.50
Candida albicans (ATCC 10231)	62.50	<31.25

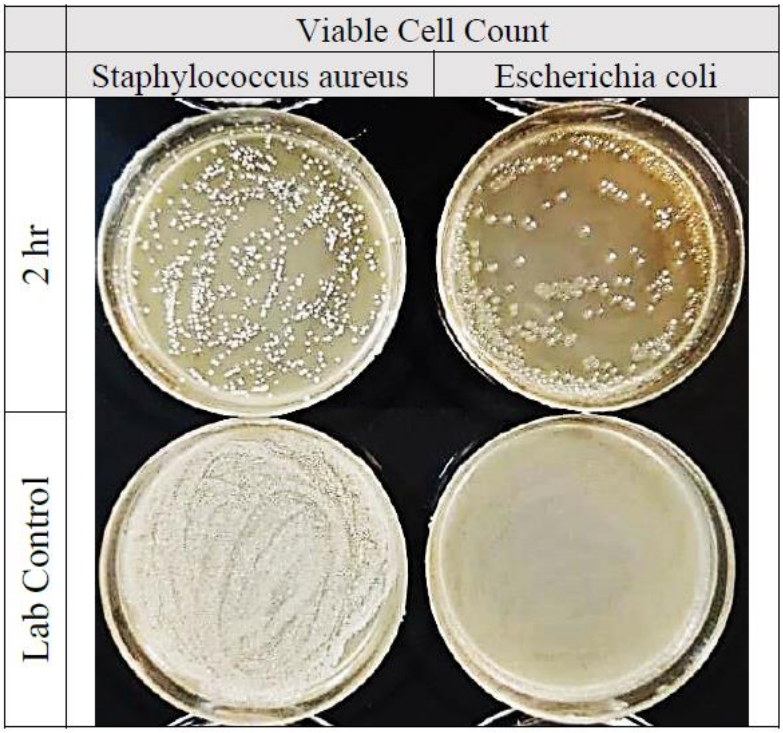

Fig. 7. Viable cell counts of cumin-loaded P/CA/SWCNT-Gl against *Escherichia coli* and *Staphylococcus aureus*.

CONCLUSIONS

In summary, this research explains the preparation and application of cumin-loaded on P/CA/SWCNT-Gl composite against bacteria. Cumin has potential to treat diseases; thus, the synthesis of cumin-carrier is a valuable strategy with positive implications for the food and cosmetic industrials. The ability of P/CA/SWCNT-Gl composite for the encapsulation of cumin and the effective parameters were studied to achieve a high yield. The best conditions for cumin encapsulation were obtained to be a low pH, 0.005 g of P/CA/SWCNT-Gl, 6 ppm of cumin, and 8 h of reaction time. Moreover, cumin-loaded P/CA/SWCNT-Gl was acted against *Escherichia coli*, *Staphylococcus aureus*, and *Candida albicans*. The excellent performance of P/CA/SWCNT-Gl suggests that it can be used as an efficient biocomposite for the essential oil-carrier by using green materials.

CONFLICT OF INTEREST

The authors declare no conflicts of interest.

REFERENCES

1. Fernández-López J, Viuda-Martos M. Introduction to the Special Issue: Application of Essential Oils in Food Systems. Foods [Internet]. 2018; 7(4). 10.3390/foods7040056
2. Burt S. Essential oils: their antibacterial properties and potential applications in foods—a review. International Journal of Food Microbiology. 2004;94(3):223-53. https://doi.org/10.1016/j.ijfoodmicro.2004.03.022
3. Amiri A, Mousakhani-Ganjeh A, Amiri Z, Guo Y-g, Pratap Singh A, Esmaeilzadeh Kenari R. Fabrication of cumin loaded-chitosan particles: Characterized by molecular, morphological, thermal, antioxidant and anticancer properties as well as its utilization in food system. Food Chemistry. 2020;310:125821. https://doi.org/10.1016/j.foodchem.2019.125821
4. Kfoury M, Auezova L, Greige-Gerges H, Fourmentin S. Encapsulation in cyclodextrins to widen the applications of essential oils. Environmental Chemistry Letters. 2019;17(1):129-43. 10.1007/s10311-018-0783-y
5. Liakos I, Rizzello L, Scurr DJ, Pompa PP, Bayer IS, Athanassiou A. All-natural composite wound dressing films of essential oils encapsulated in sodium alginate with antimicrobial properties. International Journal of Pharmaceutics. 2014;463(2):137-45. https://doi.org/10.1016/j.ijpharm.2013.10.046
6. Paseta L, Simón-Gaudó E, Gracia-Gorría F, Coronas J. Encapsulation of essential oils in porous silica and MOFs for trichloroisocyanuric acid tablets used for water treatment in swimming pools. Chemical Engineering Journal. 2016;292:28-34. https://doi.org/10.1016/j.cej.2016.02.001
7. Shetta A, Kegere J, Mamdouh W. Comparative study of encapsulated peppermint and green tea essential oils in chitosan nanoparticles: Encapsulation, thermal stability, in-vitro release, antioxidant and antibacterial activities. International Journal of Biological Macromolecules. 2019;126:731-42. https://doi.org/10.1016/j.

ijbiomac.2018.12.161
8. Sudha N, Yousuf S, Israel EVMV, Paulraj MS, Dhanaraj P. On the accessibility of surface-bound drugs on magnetic nanoparticles. Encapsulation of drugs loaded on modified dextran-coated superparamagnetic iron oxide by β-cyclodextrin. Colloids and Surfaces B: Biointerfaces. 2016;141:423-8. https://doi.org/10.1016/j.colsurfb.2016.02.020
9. Valenti D, De Logu A, Loy G, Sinico C, Bonsignore L, Cottiglia F, et al. Liposome-Incorporated Santolina Insularis Essential Oil: Preparation, Chracterization and in Vitro Antiviral Activity. Journal of Liposome Research. 2001;11(1):73-90. 10.1081/LPR-100103171
10. Ali Akbari Ghavimi S, Ebrahimzadeh MH, Solati-Hashjin M, Abu Osman NA. Polycaprolactone/starch composite: Fabrication, structure, properties, and applications. Journal of Biomedical Materials Research Part A. 2015;103(7):2482-98. https://doi.org/10.1002/jbm.a.35371
11. Mutmainna I, Tahir D, Lobo Gareso P, Ilyas S. Synthesis composite starch-chitosan as biodegradable plastic for food packaging. Journal of Physics: Conference Series. 2019;1317(1):012053. 10.1088/1742-6596/1317/1/012053
12. Wang J, Jiang X, Guo Z, Zheng B, Zhang Y. Insights into the multi-scale structural properties and digestibility of lotus seed starch-chlorogenic acid complexes prepared by microwave irradiation. Food Chemistry. 2021;361:130171. https://doi.org/10.1016/j.foodchem.2021.130171
13. Jain SK, Dutta A, Kumar J, Shakil NA. Preparation and characterization of dicarboxylic acid modified starch-clay composites as carriers for pesticide delivery. Arabian Journal of Chemistry. 2020;13(11):7990-8002. https://doi.org/10.1016/j.arabjc.2020.09.028
14. Xie J, Huang L, Wang R, Ye S, Song X. Novel visible light-responsive graphene oxide/Bi2WO6/starch composite membrane for efficient degradation of ethylene. Carbohydrate Polymers. 2020;246:116640. https://doi.org/10.1016/j.carbpol.2020.116640
15. Abasalizadeh F, Moghaddam SV, Alizadeh E, akbari E, Kashani E, Fazljou SMB, et al. Alginate-based hydrogels as drug delivery vehicles in cancer treatment and their applications in wound dressing and 3D bioprinting. Journal of Biological Engineering. 2020;14(1):8. 10.1186/s13036-020-0227-7
16. Pettignano A, Aguilera DA, Tanchoux N, Bernardi L, Quignard F. Chapter 17 - Alginate: A Versatile Biopolymer for Functional Advanced Materials for Catalysis. In: Albonetti S, Perathoner S, Quadrelli EA, editors. Studies in Surface Science and Catalysis. 178: Elsevier; 2019. p. 357-75. https://doi.org/10.1016/B978-0-444-64127-4.00017-3
17. Sahoo DR, Biswal T. Alginate and its application to tissue engineering. SN Applied Sciences. 2021;3(1):30. 10.1007/s42452-020-04096-w
18. Szekalska M, Puciłowska A, Szymańska E, Ciosek P, Winnicka K. Alginate: Current Use and Future Perspectives in Pharmaceutical and Biomedical Applications. International Journal of Polymer Science. 2016;2016:7697031. 10.1155/2016/7697031
19. Qin Y, Jiang J, Zhao L, Zhang J, Wang F. Chapter 13 - Applications of Alginate as a Functional Food Ingredient. In: Grumezescu AM, Holban AM, editors. Biopolymers for Food Design: Academic Press; 2018. p. 409-29. https://doi.org/10.1016/B978-0-12-811449-0.00013-X
20. Gao X, Guo C, Hao J, Zhao Z, Long H, Li M. Adsorption of heavy metal ions by sodium alginate based adsorbent-a review and new perspectives. International Journal of Biological Macromolecules. 2020;164:4423-34. https://doi.org/10.1016/j.ijbiomac.2020.09.046
21. Jha R, Singh A, Sharma PK, Fuloria NK. Smart carbon nanotubes for drug delivery system: A comprehensive study. Journal of Drug Delivery Science and Technology. 2020;58:101811. https://doi.org/10.1016/j.jddst.2020.101811
22. Mallakpour S, khodadadzadeh L. Ultrasonic-assisted fabrication of starch/MWCNT-glucose nanocomposites for drug delivery. Ultrasonics Sonochemistry. 2018;40:402-9. https://doi.org/10.1016/j.ultsonch.2017.07.033
23. Chegeni M, Rozbahani ZS, Ghasemian M, Mehri M. Synthesis and application of the calcium alginate/SWCNT-Gl as a bio-nanocomposite for the curcumin delivery. International Journal of Biological Macromolecules. 2020;156:504-13. https://doi.org/10.1016/j.ijbiomac.2020.04.068
24. Mallakpour S, Soltanian S. Vitamin C functionalized multi-walled carbon nanotubes and its reinforcement on poly(ester-imide) nanocomposites containing L-isoleucine amino acid moiety. Composite Interfaces. 2016;23(3):209-21. 10.1080/09276440.2016.1127723
25. Singh M, Garg M. Perlite-based building materials — a review of current applications. Construction and Building Materials. 1991;5(2):75-81. https://doi.org/10.1016/0950-0618(91)90004-5
26. Jahanshahi R, Akhlaghinia B. Expanded perlite: an inexpensive natural efficient heterogeneous catalyst for the green and highly accelerated solvent-free synthesis of 5-substituted-1H-tetrazoles using [bmim]N3 and nitriles. RSC Advances. 2015;5(126):104087-94. 10.1039/C5RA21481E
27. Demirçivi P. Synthesis and characterization of Zr(IV) doped immobilized cross-linked chitosan/perlite composite for acid orange II adsorption. International Journal of Biological Macromolecules. 2018;118:340-6. https://doi.org/10.1016/j.ijbiomac.2018.06.065
28. Chegeni M, Mehri M, Dehdashtian S, Hosseini M. Preparation and Characterization of Perlite/Starch/SWCNT-Glucose Bionanocomposite for Pathogen Detection**. ChemistrySelect. 2021;6(16):4019-27. https://doi.org/10.1002/slct.202004625
29. Giannouri M, Kalampaliki T, Todorova N, Giannakopoulou T, Boukos N, Petrakis D, et al. One-Step Synthesis of TiO_2/Perlite Composites by Flame Spray Pyrolysis and Their Photocatalytic Behavior. International Journal of Photoenergy. 2013;2013:729460. 10.1155/2013/729460